Appl. Phys. A 74, 467–474 (2002) / Digital Object Identifier (DOI) 10.1007/s003390101139

Applied Physics A
Materials
Science & Processing

A model for the interaction of near-infrared laser pulses with metal powders in selective laser sintering

P. Fischer[1,*], **N. Karapatis**[2], **V. Romano**[1], **R. Glardon**[2], **H.P. Weber**[1]

[1] Institute of Applied Physics, Laser Materials Processing, University of Bern, 3012 Bern, Switzerland
[2] Center for Advanced Rapid Tooling, Mechanical Engineering Department, Swiss Federal Institute of Technology, 1015 Lausanne, Switzerland

Received: 26 July 2001/Accepted: 23 November 2001/Published online: 23 January 2002 –

Abstract. A thermal model of the interaction of pulsed near-infrared laser radiation from a Nd:YAG laser was made, taking the measured powder properties such as reflectance, optical penetration depth and thermal conductivity into account. It allows an estimation of the evolution of two different temperatures: the average temperature of the powder (taken over the grains in a volume given by the laser beam diameter and the optical penetration depth) and the temperature distinction within a single grain. It showed that in pulsed mode consolidation can be achieved at much lower average power as the surface of the powder particles are molten but their cores remain at nearly room temperature. This leads to a much lower average temperature and therefore a dramatic decrease in residual thermal stresses in the finished piece. The results of the model were experimentally tested and confirmed.

PACS: 42.62.C; 81.20.E; 72.15.E; 07.05.T

Selective laser sintering (SLS) is a technique used to rapidly manufacture 3D parts in a layer-by-layer way in rapid prototyping and rapid manufacturing [1].

A laser beam that scans the surface of a loose powder bed, following the geometry of a sliced CAD file consolidates the freeform. Then a further layer of the powder is added, and the next layer is sintered. This technique is very promising as almost any 3D shape can be produced, without the need of prefabrication of part-specific tools [2]. Furthermore, the layer-by-layer build-upprocess allows the introduction of material-property variations or even changes to the material composition itself.

A very promising application of SLS is the precise production of implants, made of bio-compatible materials for prostheses, as the diagnostic and imaging tools used in medical applications already deliver layer-by-layer data from the human body [3].

In most applications, consolidation is performed with a high-power, continuous-wave CO_2 laser. In this case the powder is nearly homogeneously heated and sintered [6]. In this work, another approach is chosen, where near-infrared, pulsed-laser radiation is used, as it promises several advantages. Those are the possibility of a higher lateral precision due to its smaller wavelength and an easier handling of the laser source itself. Furthermore, Nd:YAG lasers are easily Q-switched, delivering pulses in the 100 ns range at repetition rates of 1–25 kHz. This way, sintering is achieved at moderate laser powers, typically below 10 W [4]. Furthermore, when using pulses of about 100 ns duration, the sintering process will take place in a totally different manner. In this paper, the effects of the 100 ns pulses on sintering are addressed.

With our set-up, the sintering process can be classified into two different domains, according to the repetition rates:

- The low repetition rate / high single pulse energy domain. In this case, the energy per pulse is sufficient to melt a narrow skin layer of the surface with only one pulse. The strong recoil effect, which can blow the powder away before any consolidation can take place, is problematic in this case.
- The high repetition rate / low single pulse energy domain. Here the amount of deposited energy per pulse is far too low to reach the melting temperature. Therefore a superposition of many pulses is required. This behaviour is similar to continuous-wave sintering, as the temperature rise per pulse is so low that temperature homogenisation can occur between two pulses. Therefore high average powers (typically 50–100 W) are required to achieve consolidation in a suitable processing time.

The high repetition rate domain can be optimised in such a manner that, although the temperature rise after one pulse is not sufficient to melt the surface layer, only a small number of pulses is required to achieve melting. In this case, the temperature-rise difference between skin temperature, ΔT_{skin}, and average temperature, ΔT_{av}, is large enough to momentarily achieve melting temperature in only a narrow skin layer, without blasting the powder away. An average power of typically one order of magnitude less (about 5 W) is required to achieve consolidation.

In this paper, this optimised situation is investigated. As the energy per pulse at the same average power is dependent

*Corresponding author.
(Fax: +41-31/631-3765, E-mail: fischer@iap.unibe.ch)

on the repetition rate, so is the maximum achieved surface temperature. This temperature rise per pulse should be high enough (more than 100 K) to achieve a sufficiently large difference between sphere surface temperature and the temperature of the surrounding powder. Then only the surfaces of the powder grains are molten and connected. This allows a predetermined density (or porosity) to be achieved, ranging from 60% to more than 90% bulk density.

The laser source used is a commercially available, Q-switched Nd:YAG laser with 5 W average power and pulses of 150 ns (FWHM) duration. To achieve the best precision possible, the powder properties such as optical and thermal behaviours should be well known, because these values influence both lateral and depth precision.

1 Model

1.1 Concept

The model describes the interaction of a laser beam with a metal powder. The incident angle of the laser beam is normal to the powder bed surface. The radiation penetrates the powder bed over a distance of several powder-sphere diameters. This optical penetration depth is determined by both the intrinsic powder material properties and the grain-size distribution. We assume that multiple scattering leads to a nearly homogenous distribution of the radiation in the powder bed, leading to almost normal incidence of the radiation on the surface of the single grains in the underlying layers. The interaction depth of the radiation with the grains is determined by either the optical penetration depth (OPD) of the bulk material (in the case of sub-picosecond laser pulses this would be only several nanometers) or the heat diffusion length (in the case of nanosecond laser pulses this would be in the range of a few micrometers).

In an initial step the laser energy heats and melts a thin skin on the surface of the individual powder particles of a thickness of a few micrometers. Hereby enough liquid is produced to achieve liquid-phase sintering with an interparticle connection coming into existence due to the minimisation of the surface energy. As the cores of the spheres are at a much lower temperature, they act as heat sinks. Only the surface of the powder spheres is molten, and therefore their cores remain mainly in their original crystalline constitution.

The average temperature is then reached after the sintering has already taken place; this is in contrast to continuous-wave laser sintering, where the average temperature determines whether sintering takes place or not. Thus in the pulsed case the average temperature is much lower than the peak skin temperature and could therefore lead to a dramatic decrease in the residual stresses of the finished piece. At the same time, far less energy is needed for this procedure.

1.2 Temperature evolution

After thermalization of the electromagnetic energy coupled into the electrons of the sphere's surface layer has taken place, the following two thermal domains must be distinguished:

– the individual particle, considered as a dense material (where the bulk values of the thermal conductivity, heat capacity, density and OPD are of importance);
– the surrounding powder, approximated by a low-diffusivity continuum (with the measured physical properties such as thermal conductivity and density).

On this basis, the following two distinct temperatures can be considered, as illustrated in Fig. 1:

– the particle skin temperature (surface at r_{sphere});
– the powder average temperature (area where $r > r_{\text{sphere}}$).

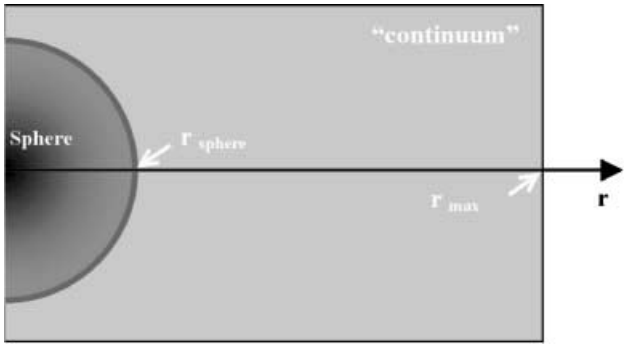

Fig. 1. Considered geometry for the described model

1.2.1 Skin temperature. In pulsed interaction mode, the temperature of a particle skin can be temporarily much higher than the average temperature. Consolidation occurs after a sufficient amount of liquid is produced. If the skin temperature clearly exceeds the melting temperature of the bulk material, liquid-phase sintering takes place, leading to a connection of the surfaces of neighbouring spheres.

1.2.2 Average temperature. The average temperature describes the temperature averaged over the whole interacting volume and is important for the thermally induced stresses of the finished piece. In pulsed mode the average temperature is much lower than the skin temperature, which allows sintering at a much lower average power, if the pulse lengths are chosen so that only a small layer of the spheres are temporarily molten. The average temperature in this case is much lower than in the continuous-wave sintering case.

1.3 Model implementation

The heat flow equation is

$$\varrho C \frac{\partial T}{\partial t} - \vec{\nabla} \cdot (k \cdot \vec{\nabla} T) = f \,, \tag{1}$$

where ϱ is the density, C the heat capacity, k the thermal conductivity and f the heat source. Transforming this equation into spherical coordinates and using spherical symmetry, the problem becomes independent of both angles ϑ and φ, and the equation to consider is

$$\varrho C \frac{\partial T}{\partial t} - \frac{1}{r^2} \frac{\partial}{\partial r} \left(r^2 \cdot k \frac{\partial T}{\partial r} \right) = f \,. \tag{2}$$

The laser pulses interacting with the powder determine the heat source, f. We chose the boundary conditions to be

$$\left. \frac{\partial T}{\partial r} \right|_{r=0} = \left. \frac{\partial T}{\partial r} \right|_{r=r_{\max}} = 0 \,, \tag{3}$$

which is warrantable if the area of simulation (r_{max}) is large enough that heat reaching its border produces a negligible temperature rise. The value at $r = 0$ is at the center of the sphere. Therefore the derivation vanishes when the sphere is homogeneously irradiated.

2 Numerical simulation

The model described in Sect. 1 was numerically solved with the implementation of the finite-difference-method solution of the heat equation noted above. The convergence criteria indicated that $\Delta r = 100\,\text{nm}$ and $\Delta t = 500\,\text{ps}$ is sufficient for a description of the heat flow when the energy is deposited with 150 ns (FWHM) pulses, whereas for shorter pulses $\Delta r = 10\,\text{nm}$ and $\Delta t = 20\,\text{ps}$ are required. The simulated material is titanium with heat diffusivities of $\kappa_{bulk} = 9.3 \times 10^{-6}\,\text{m}^2/\text{s}$ and $\kappa_{powder} = 1.48 \times 10^{-6}\,\text{m}^2/\text{s}$.

2.1 Results

All calculations show that in pulsed-laser sintering the peak skin temperature reached is significantly higher than the average temperature. This effect is more pronounced the shorter the pulses are, and the more energy the pulses contain.

Figure 2 shows the heat diffusion of a titanium sphere of radius 11 μm after interaction with a 150-ns pulse at a repetition rate of 5 kHz. The average power of the laser is 3 W, and the beam diameter is 100 μm. At the end of the pulse, the temperature of the skin is increased by a maximum temperature rise, ΔT, of 114 K, which is then subsequently efficiently cooled by the inner part of the sphere.

Figure 3 shows the evolution of the skin and center temperatures of the sphere interacting with a laser at an average power of 3 W but with different repetition rates. Figure 3a shows the case with a 5-kHz repetition rate. The two graphs show the skin temperature rise and the temperature rise at the center of the sphere. The peak skin temperature rise, ΔT, is 114 K. Figure 3b shows the results of the interaction with 15 kHz. Here ΔT is 38 K, which is three times lower than that when working with 5 kHz, as the energy per pulse is three times lower at 15 kHz, with the same average power. According to this, ΔT in Fig. 3c, which presents the case with a 25-kHz repetition rate, is 22 K.

Initially the heat flow into the sphere is much more efficient than the heat flow into the surrounding powder. This is due to the lower heat diffusivity, κ, of the powder ($\kappa_{bulk} = 9.3 \times 10^{-6}\,\text{m}^2/\text{s}$, $\kappa_{powder} = 1.48 \times 10^{-6}\,\text{m}^2/\text{s}$). It is visible that after 1.7 μs (where the two curves cross) the whole sphere is at a homogeneous temperature of 24 K above room temperature with a 5-kHz repetition rate (8 K at 15 kHz, 5 K at 25 kHz). After this time the surrounding powder acts as

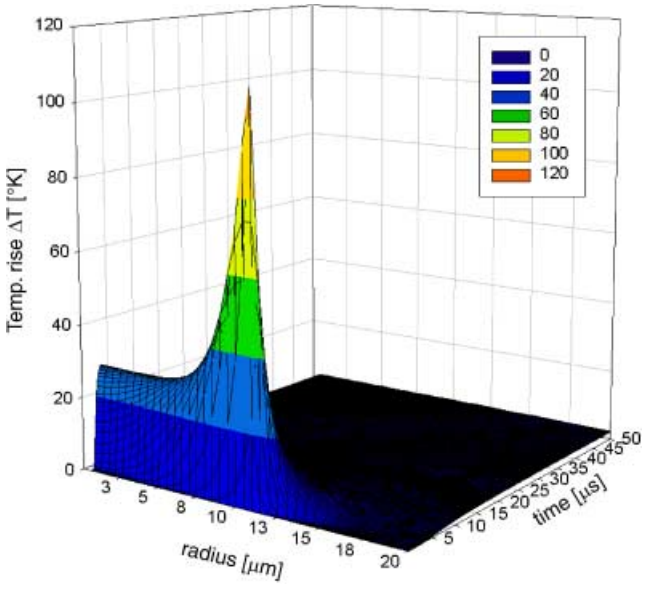

Fig. 2. Heat diffusion after a 150-ns (FWHM) pulse was deposited on the surface of a titanium sphere (11-μm radius), surrounded by titanium powder

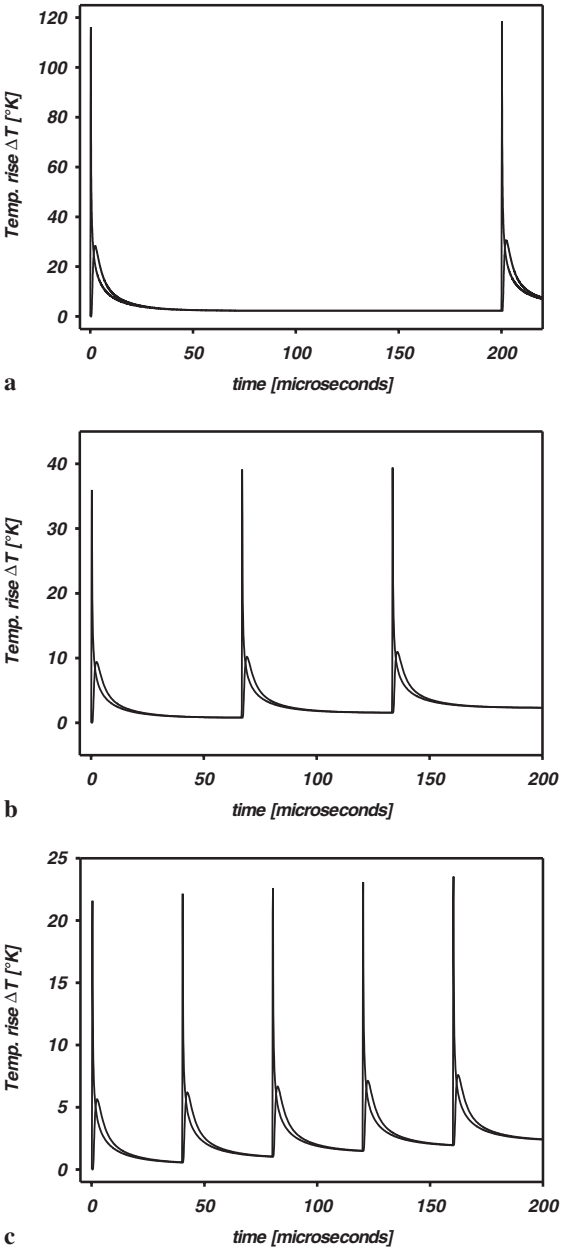

Fig. 3a–c. Evolution of skin (*higher peaks*) and center (*lower peaks*) temperatures of a 22-μm diameter titanium sphere interacting with a laser of 3 W average power at different repetition rates: **a** 5 kHz; **b** 15 kHz; **c** 25 kHz

a heat sink for the sphere. The surface is cooled faster than the center of the sphere because there is no thermal gradient within the sphere. The skin and center powder temperature rises approach the temperature of the surrounding powder before the next pulse interacts.

After 200 μs, which is the period of the pulses at 5 kHz, the same amount of energy has been deposited at all the repetition rates considered here. One can see that at this time, at all the repetition rates, the temperature rises are at nearly the same value of less than 5 K.

From Table 1 it is clear that only sintering at the low repetition rate of 5 kHz leads to a significantly different temperature development of the individual sphere and the surrounding powder. After 1.7 μs, when the center and the surface of the sphere are at the same temperature, at 15 and 25 kHz the temperatures are already at nearly the value they will reach after 200 μs, whereas at 5 kHz the temperature is more than five times higher.

The successive temperature development for many shots is shown in Fig. 4. Figure 4a shows the effect of the first 20 pulses (a time period of 40 ms) on the temperature rises. The nearly linear increase in both average and peak skin temperature is clearly visible. The linear regression leads to a time-dependent temperature rise of the powder:

$$\Delta T(t) = s \cdot t \,, \tag{4}$$

where $s = 1.2 \times 10^4$ [K/s] is the basic slope and t the time starting from the first pulse (Fig. 4a,b).

This powder temperature rise, ΔT, is identical for the repetition rates between 5 and 25 kHz, because it is determined by the total amount of deposited energy; the heat diffusion into the powder bed is too slow. After an interaction time of 0.1 s the powder temperature is 1200 K above room temperature for all cases. However, the difference between the repetition-rate domains is determined by the peak skin temperature rise per pulse, Π, which is superimposed on the base level (4). This peak skin temperature rise is 114 K when sintering at 5 kHz and 22 K at 25 kHz, which is illustrated in Fig. 5.

Thus the peak skin temperature rise, ΔT_{peak}, after time t can be written as

$$\Delta T_{\text{peak}}(t) = 1.2 \times 10^4 t + \Pi \,. \tag{5}$$

At 5 kHz and an interaction time of 0.1 s, $\Delta T_{\text{peak}} = 1314$ K, whereas it is only 1222 K at 25 kHz, which is nearly 100 K less.

The interaction time of the laser beam with the powder can be set by moving the beam across the powder bed. The time needed for the beam to travel across its own diameter is then the same time one single grain interacts with the laser radiation. With a spot size of 100 μm on the powder bed, the interaction time of 0.1 s can be achieved with a scan velocity of 1 mm/s.

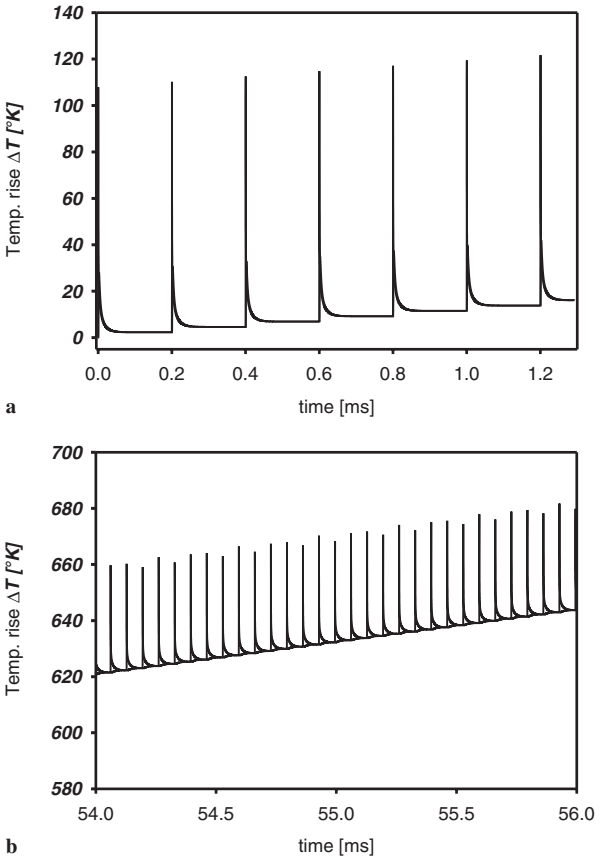

Fig. 4a,b. Temperature development during the occurrence of the first pulses of the interaction at **a** 5 kHz and **b** 15 kHz

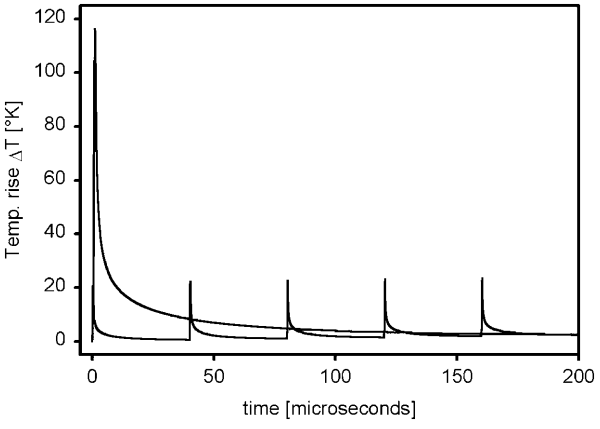

Fig. 5. Comparison of 5 kHz and 25 kHz repetition rates. The amount of deposited energy and the pulse duration are the same in both cases

Table 1. Summary of some calculated temperature rise values (in K) depicted in Fig. 3

	5 kHz	15 kHz	25 kHz
Peak skin temp. rise per pulse: Π	114 K	38 K	22 K
Average sphere temp. rise after 1.7 μs	24 K	8 K	5 K
No. of pulses in 200 μs	1	3	5
Powder temp. rise after 200 μs	< 5 K	< 5 K	< 5 K

2.1.1 Numerical simulation of sintering with shorter pulses. As the calculations have shown that a short pulse interaction is favourable for laser sintering, the case of 150-ps (FWHM) pulses at a repetition rate of 5 kHz was simulated

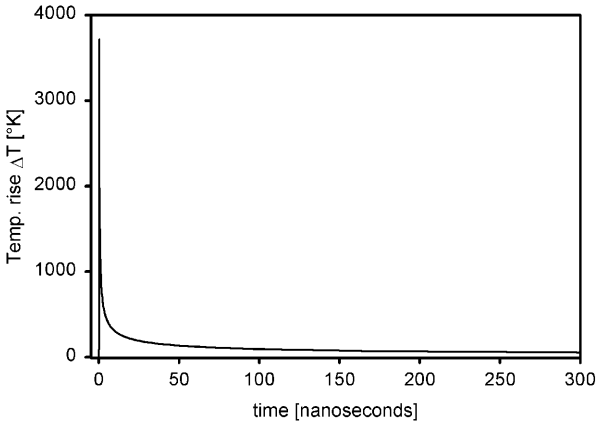

Fig. 6. Skin temperature development after the interaction of a 150-ps (FWHM) pulse with the sphere

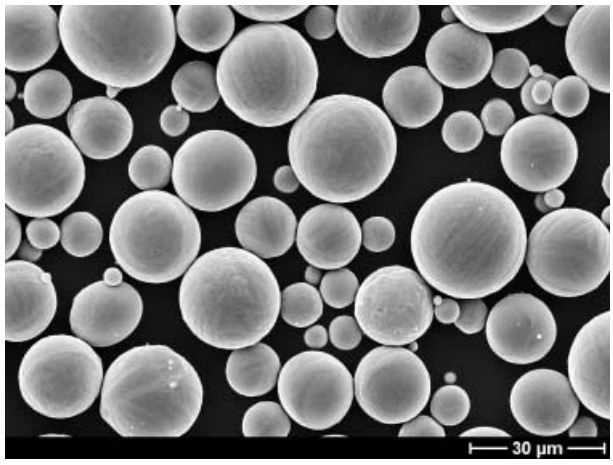

Fig. 7. SEM image of the unsintered spherical CP titanium powder

as well. For this case, the numerical simulation has to be done with smaller elements ($\Delta r = 10$ nm) and therefore also with shorter time intervals (20 ps). The results are pictured in Fig. 6. In this case, the energy would be deposited in a narrow surface layer, without any mentionable heat diffusion during the pulse duration. As can be seen in Fig. 6, this would lead to a very high peak skin temperature rise (above 3700 K, when melt enthalpy is not taken into account), which would be sufficient to melt the surface layer after only one pulse. The cooling in this case would also be very fast; after 100 ns the surface would be at only 96 K above room temperature. The calculations show that again after 1.7 µs the skin and center temperatures are at the same value (22 K above room temperature).

So with this laser source the effect of different temperature values described in the model would be very pronounced and efficient pulsed laser sintering would be possible, avoiding thermal stresses and bending of the finished green part. The resulting connection surfaces between the spheres would, however, also be much smaller, as the depths of the molten surfaces are smaller. Further, working with such a high energy per pulse, the unsintered powder would probably be blasted away from the powder bed before any connection between the grains can build up. This recoil effect has been experimentally observed at much lower pulse energies.

3 Experiments

The model was experimentally verified with the setup described in the following.

3.1 Powder characteristics [6]

A commercially pure (CP) titanium powder, provided by Pyrogenesis Co., was used to validate the model presented in this study. The titanium particles are spherical (Fig. 7), and their grain sizes have a Gaussian distribution with the mean value near 8 µm and a maximum grain size of about 30 µm (Fig. 8).

The layer density of the Pyrogenesis titanium powder is 2931.5 kg/m^3, which is equal to a volume ratio of 64.6% compared to bulk titanium (density of 4540 kg/m^3).

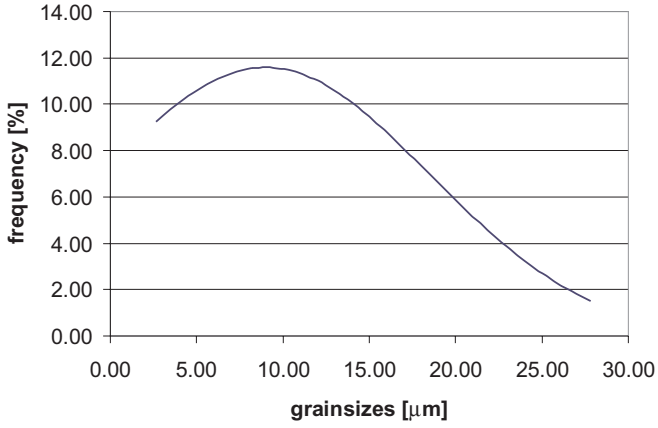

Fig. 8. Grain-size distribution of the spherical CP titanium powder

3.1.1 Optical properties. The amount of the back-scattered radiation interacting with the titanium powder measured using integrating Ulbricht spheres was found to be 70% for the Pyrogenesis titanium powder.

The optical penetration depth (OPD, defined as the depth where the intensity of the radiation is at $\frac{1}{e}$ of the non-back-scattered intensity of the Nd:YAG radiation) for the Pyrogenesis titanium powder was measured to be 63 µm. Figure 9 shows that consolidation due to liquid-phase sintering only occurs within the OPD. The underlying powder is consolidated through the well-known caking phenomenon.

The OPD of the bulk material, which becomes relevant in the interaction of each single grain at ultrashort laser pulses with near-infrared radiation (1.064 µm), is 6 nm for titanium.

3.1.2 Thermal properties. The thermal conductivity, k, of the titanium powder is a key parameter as the heat diffusivity value, $\kappa = k/\varrho C$ (where ϱ is the density of the powder and C its heat capacity), controls temperature evolution in the powder.

The thermal conductivity of the titanium powder measured in this study is $k_{\text{titanium powder}} = 1.45$ W/m K. For comparison, the thermal conductivity of other powders with similar grain-size distributions were also assessed: values

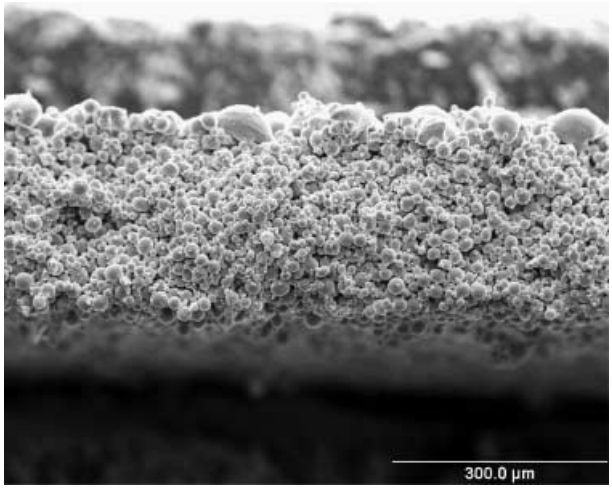

Fig. 9. Sintered titanium plate. The thickness of the molten area on the upper edge is about 60 µm, representing the optical penetration depth (OPD)

for a nickel powder and a tungsten–carbide–cobalt powder are $k_{\text{nickel powder}} = 1.23\,\text{W/m K}$ and $k_{\text{WC-12Co powder}} = 1.46\,\text{W/m K}$. These values are all in the same range, comparable to the thermal conductivity of glass, even though the values for bulk material range from 20 W/m K for titanium, to 80 W/m K for WC-12Co to 90 W/m K for nickel. Thus the grain-size distribution and the number of contacts (coordination number) seems to play a major role in the determination of the thermal properties, much more than the material itself.

3.1.3 Summary of powder characteristics. Table 2 shows a summary of the powder characteristics.

3.2 Laser parameters

The interaction of a pulsed Nd:YAG laser source (wavelength: 1.064 µm; pulse duration: 100–700 ns) with the CP titanium powder was investigated.

The deposited energy per pulse in the interaction volume,

$$V_{\text{int}} = \pi \cdot \left(\frac{\varnothing_{\text{spot}}}{2}\right)^2 \cdot \text{OPD}\,, \tag{6}$$

is given by

$$E_{\text{pulse}} = (1-R)\frac{P_{\text{av}}}{f_{\text{rep}}}\left(1-\frac{1}{\text{e}}\right)\,, \tag{7}$$

where R is the reflectivity, P_{av} the average laser power and f_{rep} the repetition rate of the Q-switch.

To estimate the influence of one pulse on one sphere of the Pyrogenesis titanium powder, the bulk values of both OPD and thermal conductivity are the important parameters. The number of spheres in the interacting volume, V_{int} (given by the beam diameter and the OPD) is

$$\text{No. of spheres} = \frac{V_{\text{int}} \cdot \frac{\varrho_{\text{bulk}}}{\varrho_{\text{powder}}}}{V_{\text{sphere}}}\,. \tag{8}$$

By considering that the CP titanium powder interacts with a beam of 100 µm diameter and an OPD of 60 µm, the number of spheres is can be approximated to be 55, assuming only 22-µm-diameter spheres. Thus the part of the pulse energy received by each particle is

$$E_{\text{pulse}} = \frac{1-R}{\text{No. of spheres}} \cdot \frac{P_{\text{av}}}{f_{\text{rep}}} \cdot \left(1-\frac{1}{\text{e}}\right)\,. \tag{9}$$

The energy of the laser pulse of 150 ns duration (FWHM) is deposited at the surface of the powder sphere. As the heat diffusion, $z_{\text{d}}(t) = 2\sqrt{\kappa t}$ (κ is the heat diffusivity), during $t = 150$ ns is about 2.3 µm (the distance at which the temperature is at about 10% of the value at the source), most of the energy is deposited within a layer of 1-µm thickness.

3.3 Experimental setup parameters

The SLS processing setup emits Q-switched Nd:YAG laser pulses of 150 ns duration (FWHM) at repetition rates of 5 to 25 kHz and average powers of 1 to 5 W in the fundamental Gaussian TEM_{00} mode. The beam diameter on the powder surface is 100 µm, resulting in fluences ranging from 1 to 11 J/cm^2 per pulse.

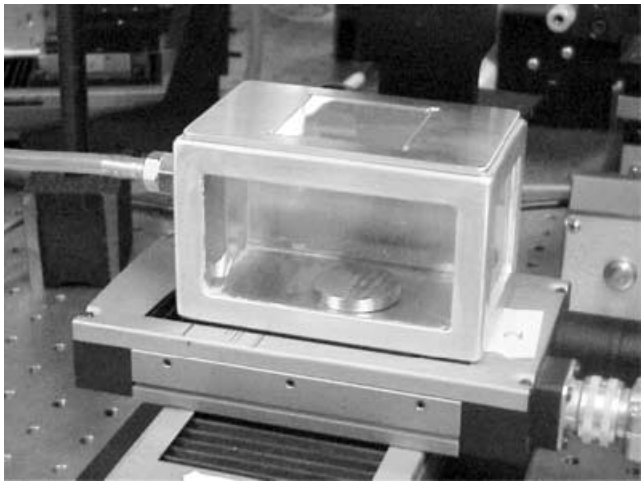

Fig. 10. x–y translation stage with gas chamber and powder on a steel substrate in an argon atmosphere

The powder bed was placed on a steel substrate in an argon atmosphere to avoid the strongly exothermic oxidation

Table 2. Summary of the powder characteristics. The volume ratio was determined by the ratio of the bulk to powder density. OPD: optical penetration depth $\left(\frac{1}{\text{e}}\right)$; k: thermal conductivity; C: heat capacity, scaled with the volume ratio; κ: thermal diffusivity, determining the heat diffusion

Powder	Volume ratio (%)	OPD (µm)	k (W/m K)	C (scaled; J/g K)	κ (10^{-6} m^2/s)
Titanium (Pyrogenesis)	64.6	60	1.45	0.335	1.481
Nickel (EMP 1126)	54.8	≤ 20	1.23	0.252	1.007

of the powder. The target was moved with a precise (1 μm) computer-controlled x–y translation stage at a scan speed of 1 mm/s (Fig. 10).

3.4 Different repetition rates at 3 W *average power*

The following sintered plates were produced at a scan speed of 1 mm/s, a beam diameter of 100 μm and a scan shift of 50 μm from line to line. Thus the overlap of two subsequent passes of the beam means that each region is treated twice.

The repetition rate influences the surface roughness. The size of the connected grains increases as the repetition rate decreases, which leads to a slightly higher surface roughness (Figs. 12, 13 and 14), as on the surface more liquid is formed due to the higher peak temperature increase, Π.

Figures 12, 13 and 14 show the sintered surface of the Pyrogenesis titanium powder. All the plates were sintered with 3–3.2 W average power, but at different repetition rates. Thus the amount of deposited energy is always in the same range, but all the pictures show different interaction behavior.

Figure 11 shows the different regions of average powers and repetition rates, leading to different types of interaction of the radiation with the titanium powder. The sintering threshold for 5 kHz is not measured yet, thus the transition line between the unsintered and sintered region is uncertain. It is visible that there is a large difference when the same amount of energy (manifested in the average power) is deposited at a repetition rate of 5 kHz or higher. But there is almost no difference between 15 kHz and 25 kHz. Figures 12, 13 and 14 show that by changing the repetition rate at the same average power level, all the three regions of Fig. 11 (molten, sintered and partially molten, weakly sintered) can be achieved.

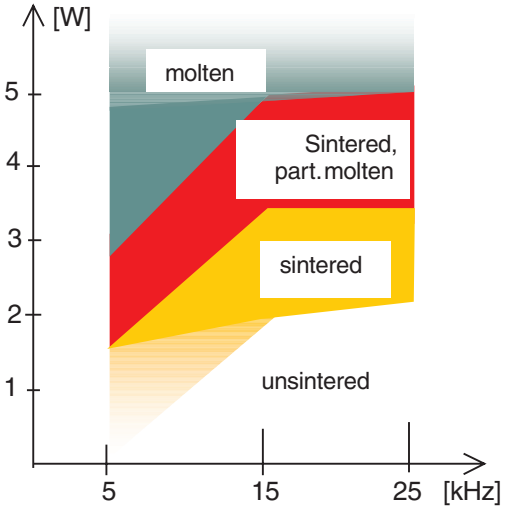

Fig. 11. Power versus repetition rate for the Pyrogenesis titanium powder

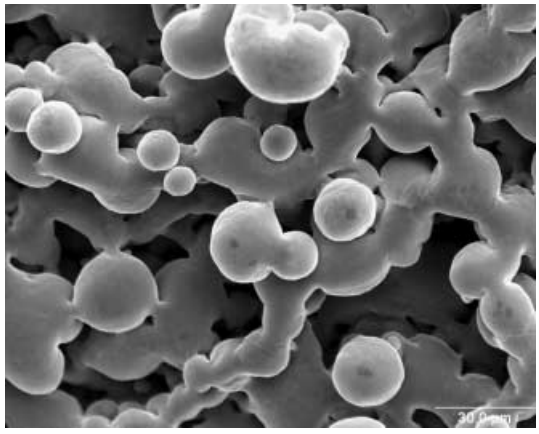

Fig. 12. Strongly sintered titanium powder. 5 kHz repetition rate, 3 W average power, 600 μJ/pulse, total 7.6 kJ/cm

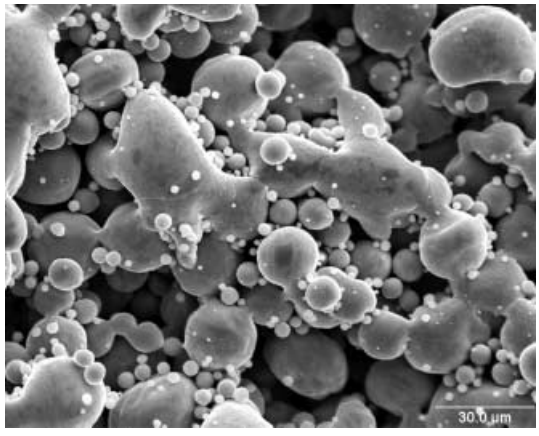

Fig. 13. Sintered titanium powder. 15 kHz repetition rate, 3.2 W average power, 210 μJ/pulse, total 8.1 kJ/cm

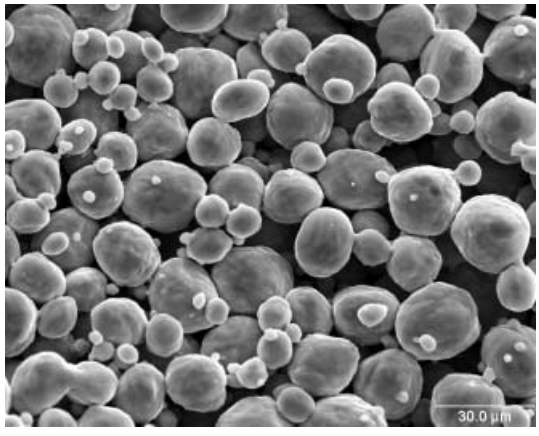

Fig. 14. Weakly sintered titanium powder. 25 kHz repetition rate, 3.2 W average power, 130 μJ/pulse, total 8.1 kJ/cm

3.4.1 Sintered plates at the parameters considered in the simulation. The total amount of the deposited energy per area is in the same range for all the plates in Figs. 12, 13 and 14, although an obvious difference occurs. At frequencies as low as 5 kHz (Fig. 12) at least the surface of all the grains are molten, and therefore the grains are connected to form a skeleton-like structure. At an increased repetition rate, always fewer grains are connected. In Fig. 14 only the small grains are molten, building bridges between the bigger grains to hold them together. Even though the deposited energy when sintering at 25 kHz is slightly bigger than the energy when sintering at 5 kHz, the thermal effect is smaller.

4 Discussion

As the 15 kHz and 25 kHz repetition rate cases only differ slightly from each other, the discussion is limited in the following to the two extreme cases of 5 kHz and 25 kHz.

5 kHz: The numerically calculated temperature rises of the surface and center of an individual sphere of 22 μm diameter and the surrounding powder showed that liquid-phase sintering can be performed at a low average power of 3 W. The maximum skin temperature rise per pulse, Π, is 114 K. After 1.7 μs the center and skin temperature have the same value of 24 K above room temperature, meaning that the sphere is homogeneously heated, whereas the surrounding powder has not yet been significantly affected by heat. Thereafter the surface of the sphere is cooled faster as the thermal gradient points towards the powder. Numerical simulation over the time needed for the laser beam to pass over its own diameter (100 μm) showed that the average temperature rise is 1200 K, while the peak skin temperature rise is 1314 K, which is sufficient for liquid-phase sintering. The experiment has shown that also the surface of the bigger spheres of the powder is molten, leading to a skeleton-like connection.

25 kHz: As the repetition rate is 5 times higher than at 5 kHz, the energy per pulse is 5 times less in the case of 25 kHz. This factor 5 is found again in the maximum skin temperature rise, which at 22 K in the case of 25 kHz is 5 times lower than in the case of 5 kHz. Also the temperature rise of the sphere after 1.7 μs, where the whole sphere is at the same temperature (5 K), is 5 times lower than compared with the 5 kHz case. The average powder temperature after 0.1 s (time needed for the laser beam to travel over its own diameter) is again 1200 K, whereas the peak skin temperature rise is 1222 K above room temperature, which is nearly 100 K less than in the case of 5 kHz. This difference seems to be big enough to only efficiently melt the surface of the smaller grains; the bigger grains stay unmelted. The smaller grains then connect the bigger grains to form a sintered plate.

5 Conclusions

The advantage of a pulsed radiation, as described in the present model is the possible distinction between the temperature of the surface of the sphere (skin temperature) and temperature of the surrounding powder (average temperature). This makes it possible to achieve laser sintering at average laser powers of less than 10 W (in the case of the titanium powder used and a spot size of 100 μm). The model and the simulation have shown that, by using even shorter laser pulses, this advantage could be used even more efficiently, as long as there is sufficient energy per pulse available. Investigations of both shorter laser pulses for the interaction and the solid-state sintering process are in progress.

Acknowledgements. The authors acknowledge funding by Swiss Federal Project CTI 4560.1. They are also grateful to Dr. B. Gasser and Dr. L. Eschbach from the foundation "Dr. h. c. Robert Mathys Stiftung", Bettlach (Switzerland), for support with materials and for fruitful discussions. Further thank goes to Dr. Duerr from Lasag AG, Thun for support and E. Kraehenbuehl for technical assistance.

References

1. J.-P. Kruth: "Rapid Prototyping, a New Application of Physical and Chemical Processes for Material Accretion Manufacturing." In: Proceedings of the 11th International Symposium for Electromachining, Lausanne (Switzerland) (Presses Polytechniques et Universitaires Romandes; EPFL Lausanne 1995) pp. 3–28
2. M. Agarwala, D. Bourell, J. Beaman, H. Marcus, J. Barlow: Rapid Prototyping Journal **1**(1), 26–36 (1995)
3. E. Berry, J.M. Brown, M. Connell, C.M. Craven, N.D. Efford, A. Radjenovic, M.A. Smith: Med. Eng. Phys. **19**, 90 (1997)
4. H.J. Niu, I.T.H. Chang: J. Mater. Sci. **35**, 31 (2000)
5. W. O'Neill, C.J. Sutcliffe, C.J. Morgan, K.K.B. Hon: "Investigation of Short Pulse Nd:YAG Laser Interaction with Stainless Steel Powder Beds." In: Proc. Solid Freeform Fabrication Symp., 1998, Austin (USA) (1998) pp. 147–160.
6. P. Fischer, V. Romano, H.P. Weber: Near infrared pulsed laser sintering of metal powders. Internal Report, University of Bern